dielectric waveguides," *Bell Syst. Tech. J.*, vol. 48, pp. 2133–2160, Sept. 1969.
[4] R. Pregla, "A method for the analysis of coupled rectangular dielectric waveguides," *Arch. Elekt. Übertragung*, band 28, pp. 349–357, Sept. 1974.
[5] A. L. Cullen and O. Ozkan, "Coupled parallel rectangular dielectric waveguides," *Proc. Inst. Elec. Eng.*, vol. 122, pp. 593–599, June 1975.
[6] J. F. Heitmann, "Theory and fabrication of dielectric image lines and measurements in the frequency range from 26.5 to 40 GHz," *NTZ-Aufsätze*, vol. 28, pp. 279–284, Aug. 1975.
[7] K. Ogusu and K. Hongo, "Analysis of dielectric waveguides by generalized telegraphist's equations," *Trans. Inst. Electron. Commun. Eng. Jap.*, (Corresp.) vol. J60-B, pp. 358–359, May 1977
[8] ——, "Experimental investigation of dispersion characteristics in rectangular dielectric waveguides," *Trans. Inst. Electron. Commun. Eng. Jap.*, to be published.
[9] J. E. Goell, "Rib waveguide for integrated optical circuits," *Appl. Optics*, vol. 12, pp. 2797–2798, Dec. 1973.
[10] H. Furuta, H. Noda, and A. Ihaya, "Novel optical waveguide for integrated optics," *Appl. Optics*, vol. 13, pp. 322–326, Feb. 1974.
[11] E. A. J. Marcatili, "Slab-coupled waveguides," *Bell Syst. Tech. J.*, vol. 53, pp. 645–674, Apr. 1974.
[12] V. Ramaswamy, "Strip-loaded film waveguide," *Bell Syst. Tech. J.*, vol. 53, pp. 697–704, Apr. 1974.
[13] D. Marcuse, "Theory of the single-material fiber," *Bell Syst. Tech. J.*, vol. 53, pp. 1619–1641, Oct. 1974.
[14] W. V. McLevige, T. Itoh, and R. Mittra, "New waveguide structures for millimeter-wave and optical integrated circuits," *IEEE Trans. Microwave Theory Tech.*, vol. MTT-23, pp. 788–794, Oct. 1975.
[15] T. Itoh, "Inverted strip dielectric waveguide for millimeter-wave integrated circuits," *IEEE Trans. Microwave Theory Tech.*, vol. MTT-24, pp. 821–827, Nov. 1976.
[16] S. A. Schelkunoff, "Generalized telegraphist's equations for waveguides," *Bell Syst. Tech. J.*, vol. 31, pp. 784–801, July 1952.
[17] N. Marcuvitz, *Waveguide Handbook*. New York: McGraw-Hill, 1951, ch. 2.

Solutions of the Vector Wave Equation for Inhomogeneous Dielectric Cylinders—Scattering in Waveguide

GABRIELE CICCONI AND CARLO ROSATELLI

Abstract—**Some solutions of the vector wave equation for an inhomogeneous dielectric cylinder, suitable for numerical calculations of the scattered electromagnetic (EM) field in waveguide, are presented in cases where the cylinder axis is parallel, or perpendicular, to the incident electric field vector. The scattered field, given in terms of normal modes of the rectangular waveguide, permits easy determination of the transmission and reflection coefficients for the structure. The dielectric susceptibility may be considered as variable along the cylinder radius according to a parabolic function (Luneberg-type profile). Finally, numerical results of the scattered near field are presented for Teflon cylinders of different diameters, in the case of parallel polarization. They are compared with laboratory measurements in the microwave *X* band made as a reliability test of the computational program. The agreement between measured and computed values is satisfactory within a deviation of 10 percent in the whole frequency band.**

I. Introduction

SCATTERING and diffraction in free space by cylindrical objects of homogeneous and stratified dielectric, when the incident electromagnetic (EM) field is parallel or perpendicularly polarized, have been investigated by various authors [1]. The inhomogeneous case has also been treated for scattering by plasma columns [2].

The same problem in waveguide has been developed both for parallel incidence, by solving the wave vector equation in the case of inhomogeneous dielectric or plasma columns [3]–[5], and for perpendicular incidence, by using variational and Green's function techniques [6], [7].

In this paper, some exact solutions of the vector wave equation, in circular cylindrical coordinates and for homogeneous and radially inhomogeneous (Luneberg-type parabolic variable profile) complex permittivities, are presented in cases of parallel and perpendicular incidences of the EM field. These solutions have been expressed in a series of tabulated Bessel functions (homogeneous dielectric case) or in a series of confluent hypergeometric or Kummer's functions (inhomogeneous parabolic case). They have been found as suitable for developing numerical calculations of microwave scattering in waveguide.

Approximate values dependent on the truncation of the field series expansion may be estimated by the unitary condition of the scattering matrix.

The numerical results concerning the scattered near field

Manuscript received November 29, 1976; revised May 23, 1977.
The authors are with the Electrical Engineering Department, University of Genoa, Genoa, Italy.

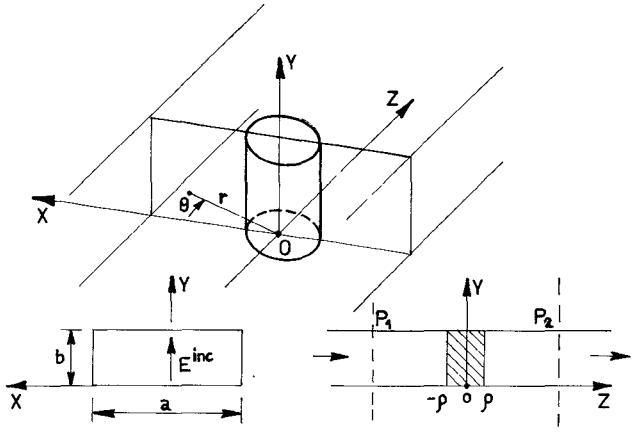

Fig. 1. The geometry of the problem.

have been obtained using Teflon cylinders which had different diameters and were placed as posts in rectangular waveguide, only when their axes were parallel to the incident electric field. These results are compared with those obtained by laboratory measurements in the microwave X band. The electric field was measured by using a slotted guide section at the center of the waveguide, within a distance of a few wavelengths from the scatterer surface, in reflection and transmission zones. In order to increase the reliability of the measurements, different types of detectors (crystal and bolometer) were used.

The agreement between measured and computed values may be considered reliable in the whole frequency band within a deviation of the order of 10 percent for both amplitudes and phases, when the complex permittivity has value of $2.06 - i10^{-5}$.

II. Theoretical Considerations

A. Solutions of the EM Field in Dielectric Cylinders

Assuming the simple harmonic time dependence $e^{i\omega t}$, the homogeneous vector wave equation in dielectric cylinders can be written as

$$\nabla x \nabla x \vec{E} - k^2 \varepsilon \vec{E} = 0 \tag{1}$$

in the domain $r \leq \rho$, $0 \leq \theta \leq 2\pi$, $0 < y < b$, where $\omega = kc$ and ε is the complex relative permittivity.

This equation is solved in cylindrical coordinates (r,θ,y) according to the geometry of Fig. 1.

We confine our attention to

$$\varepsilon = 1 - \chi_0 \left(1 - \alpha \frac{r^2}{\rho^2}\right) \tag{2}$$

where $-\chi_0$ is the axial susceptibility of the cylinder, $0 \leq \alpha \leq 1$ is an inhomogeneity parameter, and ρ is the cylinder radius. This choice is particularly suitable for describing positive columns of discharge plasmas [2] or dielectrics having permittivities of the Luneberg type.

The case of parallel incidence, where $\vec{E} = (0,0,E_y)$, was treated using a plasma inhomogeneous cylinder with a glass container [5]. In this case by applying the Fourier method (1) may be reduced to a system of two differential equations of which the one in r is a Whittaker equation [8]. This equation for $\alpha = 0$, i.e., for homogeneous dielectric, becomes a Bessel equation. The equation in θ is simply the Helmoltz equation. The solution can be written in a Fourier series as

$$E_y(r,\theta) = \sum_{m=0}^{\infty} A_m G_m(kr) \cos m\theta \tag{3}$$

with

$$G_m(kr) = \exp\left[-i\frac{(\alpha\chi_0)^{1/2}}{2k\rho}(kr)^2\right] \cdot \left[\frac{i(\alpha\chi_0)^{1/2}}{k\rho}\right]^{(m+1)/2} \cdot k(kr)^m \cdot \phi\left(\frac{m+1}{2} + i\frac{h_0 k\rho}{4(\alpha\chi_0)^{1/2}}, \frac{m+1}{2}; \frac{i\alpha(\alpha\chi_0)^{1/2}}{k\rho}(kr)^2\right)$$

where $h_0 = 1 - \chi_0$ and $\phi(a,c,x)$ is the Kummer or confluent hypergeometric function. The complex amplitudes A_m are calculated by applying the usual boundary continuity conditions for tangential electric and magnetic fields.

In the case of perpendicular incidence for the EM field, $\vec{E} = (E_r,E_\theta,0)$. Then (1) is reduced to a system of two scalar differential equations as follows:

$$\frac{1}{r^2}\frac{\partial^2 E_r}{\partial\theta^2} + \frac{\partial^2 E_r}{\partial y^2} + k^2\varepsilon E_r - \frac{1}{r^2}\frac{\partial E_\theta}{\partial\theta} - \frac{1}{r}\frac{\partial^2 E_\theta}{\partial r\,\partial\theta} = 0 \tag{4}$$

$$\frac{1}{r}\frac{\partial E_r}{\partial y} + \frac{\partial^2 E_r}{\partial r\,\partial y} + \frac{1}{r}\frac{\partial^2 E_\theta}{\partial\theta\,\partial y} = 0. \tag{5}$$

In applying the Fourier method to these equations, the following solutions written in terms of TE $(0,v)$ modes are considered:

$$E_r(r,\theta,y) = \sum_{v=1}^{\infty} R_r^v(r)\Theta_r^v(\theta) \sin\frac{v\pi}{b}y \tag{6}$$

$$E_\theta(r,\theta,y) = \sum_{v=1}^{\infty} R_\theta^v(r)\Theta_\theta^v(\theta) \sin\frac{v\pi}{b}y \tag{7}$$

where v is an integer.

In this circumstance, (4) and (5), for ε given by (2), become, respectively, a Kummer equation for $R_r^v(r)$ (which in the case of homogeneous dielectrics becomes a Bessel-type equation [8]) and a Helmoltz equation for $\Theta_r^v(\theta)$.

Hence by (5) we obtain the relation

$$R_\theta^v\Theta_\theta^v = -\left[R_r^v + r\frac{\partial R_r^v}{\partial_r}\right]\int \Theta_r^v(\theta)\,d\theta \tag{8}$$

where

$$\Theta_\theta^v = \Theta_r^v = A_p^v \cos p\theta + B_p^v \sin p\theta$$

with p as a positive real integer.

The solution for R_r may be written in the form

$$R_r^v(r) = \exp\left[-i\tfrac{1}{2}dr^2\right]r^{p-1} \cdot \left[C_p^v\phi(b_{p,v}, 1+p; idr^2) + D_p^v(idr^2)^{-p}\phi(b_{p,v}-p, 1-p; idr^2)\right] \tag{9}$$

where

$$d^2 = \frac{\alpha\chi_0}{\rho^2}k^2 \qquad b_{p,v} = \frac{1+p}{2} + \frac{ik_v^2}{4d}$$

$$k_v^2 = k^2(1-\chi_0) - \left(\frac{v\pi}{b}\right)^2.$$

The amplitudes C_p^v and D_p^v are calculated by applying the continuity conditions of the tangential fields at the cylindrical boundary surface.

B. Scattered Field in Rectangular Waveguide

The incident wave propagates along the waveguide axis in the dominant mode TE (1,0). In the case of parallel incidence to the cylinder axis, the scattered field is determined by applying the image principle [3]–[5].

In cylindrical coordinates (r,θ,y), as indicated in Fig. 1, this is written as

$$E_y^{sc}(r,\theta) = \sum_{n=0}^{\infty} B_n H_n^{(2)}(kr) \cos n\theta + \sum_{n=0}^{\infty} \sum_{\substack{p=-\infty \\ p\neq 0}}^{\infty} (-1)^p B_n H_n^{(2)}(kr_p) \cos n\theta_p \quad (10)$$

where $k = \omega/c$; r_p is the distance from $P(r,\theta)$ to 0_p, the pth image of the 0 point; θ_p is the $\widehat{r_p z}$ angle; and B_n are calculated by imposing the boundary conditions.

Equation (10) may be rewritten in a more suitable form in terms of normal modes TE $(v,0)$ of the rectangular waveguide. This goal may be attained by writing the Hankel functions in the form of the Sommerfeld integral [9]; then, by a suitable variable transformation, it is possible to use the Poisson sum formula [10]. From (10) we have

$$E_y^{sc}(x,z) = \sum_{n=0}^{\infty} \sum_{v=1}^{\infty} (\pm i)^n B_n \frac{4\varepsilon_{v,n}}{a\beta_{2v-1}} \cos\frac{(2v-1)}{a}\pi x e^{i\beta_{2v-1}|z|} \quad (11)$$

where $(+)$ is for $z > 0$ (transmission zone), $(-)$ is for $z < 0$ (reflection zone),

$$\beta_1 = \left(k^2 - \frac{\pi^2}{a^2}\right)^{1/2}$$

$$\beta_v = -i\left[\left(\frac{v\pi}{a}\right)^2 - k^2\right]^{1/2}, \qquad v > 1$$

$$\varepsilon_{1,n} = \cos\left(n \sin^{-1}\frac{\pi}{ka}\right)$$

$$\varepsilon_{v,n} = \cos\left(n\frac{\pi}{2} + in \cosh^{-1}\frac{(2v-1)\pi}{ka}\right), \qquad v > 1$$

and a is the waveguide width in the x direction.

In the case of perpendicular incidence, the scattered field is written in terms of TE $(0,v)$ modes, by neglecting TE (μ,v) (where $\mu > 0$) and TM (μ, v) modes, as follows:

$$E_x^{sc}(y,z) = \sum_{v=1}^{\infty} B_v^{(a)} \sin\left(\frac{v\pi}{b}y\right) e^{-i\beta_v z} \quad (12)$$

where $\beta_1, \beta_v (v > 1)$ are expressed in terms of the waveguide width b in the y direction and superscript (a) defines the scattering zone in waveguide ($z > 0$, transmission zone, and $z < 0$, reflection zone) for $\rho^2 < (z^2 + y^2)$. This formulation may be considered a good approximation.

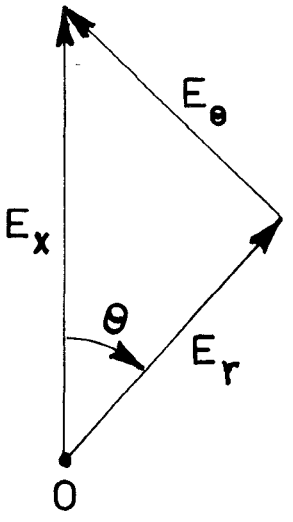

Fig. 2. Decomposition of the electric field vector (perpendicular incidence).

In cylindrical coordinates (12) may be rewritten in the form

$$E_x^{sc}(r,\theta,y) = \sum_{v=1}^{\infty} B_v \left[J_0(\beta_v r) + 2\sum_{n=1}^{\infty}\left(J_{2n}(\beta_v r)\cos 2n\theta + iJ_{2n-1}(\beta_v r)\sin(2n-1)\theta\right)\sin\frac{v\pi}{b}y\right] \quad (13)$$

where the transmission zone is defined for $0 \le \theta \le \pi$, and the reflection zone is defined for $\pi \le \theta \le 2\pi$.

C. Boundary-Value Conditions and Scattering Matrix

Our aim is to calculate the scattered Fourier amplitudes B_n by solving the boundary-value problem, along the cylinder surface, for every spectral harmonic of the field in cylindrical coordinates. Thus an inhomogeneous linear algebraic system is yielded whose dimension is dependent on the truncation index of the field series; this system is then solved using a suitable numerical technique [5], [11].

In the case of parallel polarization, boundary conditions are imposed on the tangential components of the field as follows:

$$E_y^{sc}(\rho) - E_y^{cyl}(\rho) = -E_y^{inc}(\rho)$$
$$\left.\frac{\partial E_y^{sc}(r)}{\partial r}\right|_{r=\rho} - \left.\frac{\partial E_y^{cyl}(r)}{\partial r}\right|_{r=\rho} = -\left.\frac{\partial E_y^{inc}(r)}{\partial r}\right|_{r=\rho}. \quad (14)$$

Whereas, in the case of perpendicular polarization, the scattered field is decomposed into the two orthogonal components:

$$E_r^{sc} = E_x^{sc}\cos\theta \qquad \text{and} \qquad E_\theta^{ec} = E_x^{sc}\sin\theta$$

as shown in Fig. 2.

In this case the approach to numerical computation of scattered Fourier amplitudes may be performed by choosing a given number of waveguide normal modes for every cylindrical harmonic of the field, and then by applying the moment method [12], or the extended boundary conditions (EBC) technique [13].

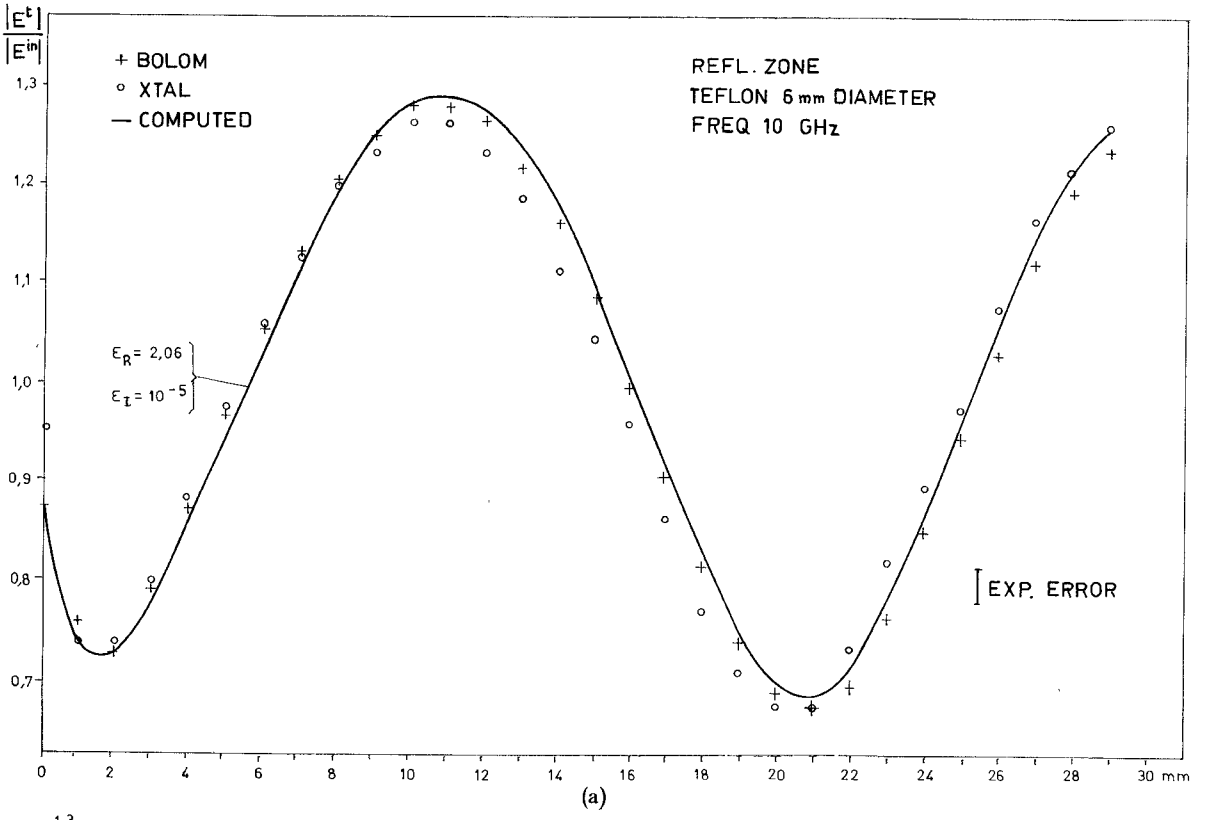

Fig. 3. Scattered total electric field versus distance from the scatterer surface. Teflon cylinder (6-mm diameter). (a) Reflection zone. (b) Transmission zone.

The linear algebraic system may be synthetically written as

$$\int_s F_j^{sc}(\rho,\theta,y)g_q(\theta)h_s(y)\,dS - \int_s F_j^{(y)}(\rho,\theta,y)g_q(\theta)h_s(y)\,dS = -\int_s F_j^{inc}(\rho,\theta,y)g_q(\theta)h_s(y)\,dS. \quad (15)$$

Here $\int_0^{\Delta V} |E^{(y)}|^2\,dV =$ finite, and the F_j are, respectively, $\varepsilon E_r, E_\theta$, just given, and H_y, which is the tangential magnetic field, calculated by Maxwell equations; $\{g_q\}$ and $\{h_s\}$ are proper function sets chosen in a suitable fashion according to the method of solution. For instance, for the EBC solution, it is possible to choose

$$\{g_q(\theta)\} = \{\cos q\theta\} \qquad \{h_s(y)\} = \left\{\sin\left(\frac{s\pi}{b}y\right)\right\}$$

with q, $s = 0, 1, 2, \cdots$ where the number of component functions depends on the number of terms of the truncated series.

The scattering matrix may be readily calculated from (11) and (13) by fixing reference planes P_1 and P_2 far from the cylinder surface, as shown in Fig. 1. The distance of these planes from the cylinder axis is chosen as an integer multiple of the wavelength in guide ($\beta_1 |z| = n2\pi$, with $n = 0, 1, 2, \cdots$).

By assuming that the propagating mode is the only dominant one ($v = 1$), the elements of the scattering matrix are

$$S_{11} = \frac{E^{sc}|_{P_1}}{E^{inc}|_{P_1}} = R \quad (16)$$

which is the reflection coefficient, and

$$S_{12} = \frac{(E^{inc} + E^{sc})_{P_2}}{E^{inc}|_{P_2}} = T \quad (17)$$

which is the transmission coefficient. The incident field at P_1 is

$$E^{inc}|_{P_1} = \cos\frac{\pi x}{a}, \qquad \text{for parallel incidence}$$

$$E^{inc}|_{P_1} = \sin\frac{\pi y}{b}, \qquad \text{for perpendicular polarization.}$$

For symmetry, the other elements are

$$S_{12} = \overline{S_{21}} \qquad \text{and} \qquad S_{22} = \overline{S_{11}}$$

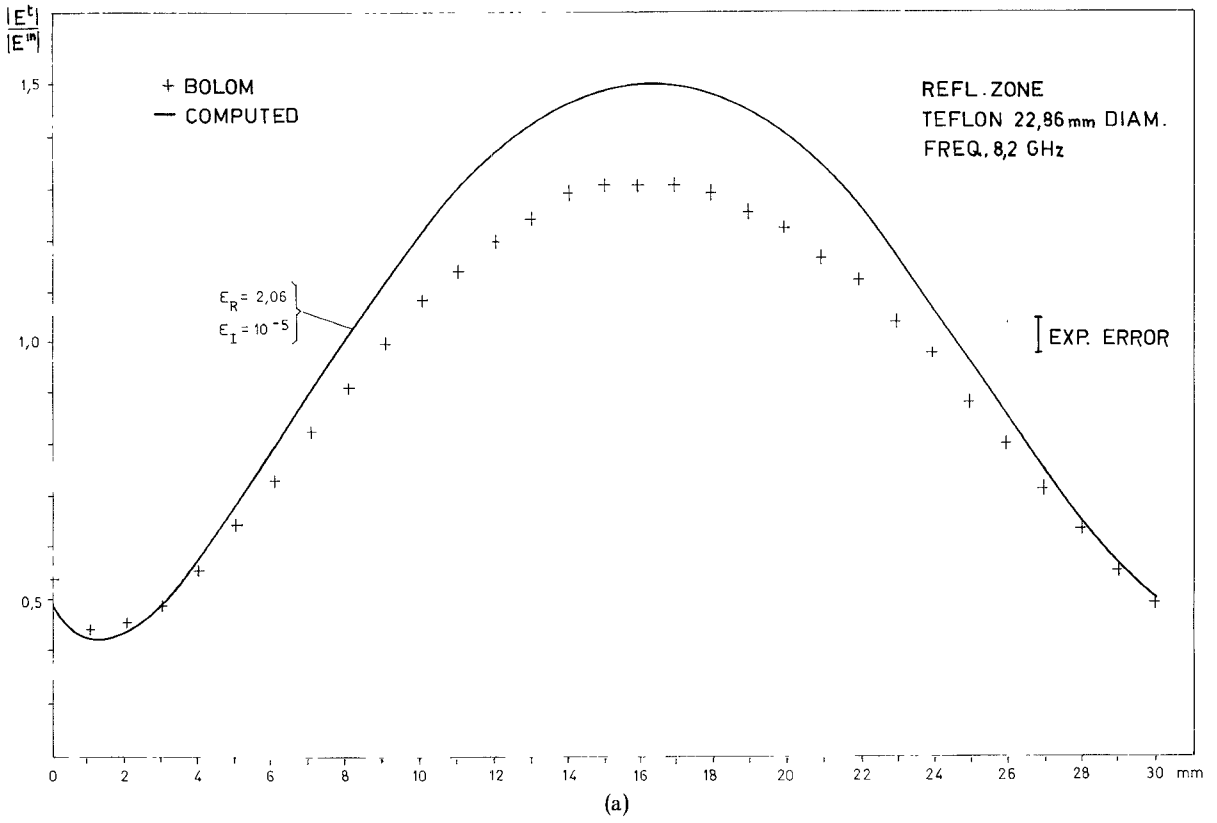

Fig. 4. Scattered total electric field versus distance from the scatterer surface. Teflon cylinder (22.86-mm diameter). (a) Reflection zone. (b) Transmission zone.

so that

$$\det S = |S_{11}|^2 + |S_{21}|^2 = |R|^2 + |T|^2 \qquad (18)$$

which, for a lossless structure, is equal to unity.

In a reference calculation for real permittivity, the error due to truncation of the field series may be evaluated by the deviation from the unitary condition.

III. Numerical Calculation and Measurements of Scattered Fields

In the case of parallel polarization, a computational program was developed for scattered field calculations [14]. In order to gain information to estimate the reliability of the computational program for (11), laboratory measurements in the microwave X band of the scattered electric field component at the center of the waveguide, along the axis, were carried out for a Teflon cylinder having two typical diameters (6 and 22.86 mm, the latter corresponding to WR 90 waveguide inner width).

In reflection and transmission zones the scattered fields were measured, using a slotted guide device from a 0.5-mm minimum distance to the cylinder surface over a length not exceeding 10 cm. Both bolometer and crystal detectors, connected to untuned electrostatic probes sliding along the waveguide and having adjustable penetration, were used for detection of the field amplitude.

In order to increase measurement accuracy and avoid nonlinear effects in detection operation due to amplitude excursion of the measured field along the waveguide, the detector current was kept constant by adjusting the level of the microwave standard source through a variable precision attenuator.

The maximum deviation of the measured values obtained by crystal and bolometer rectifiers, due essentially to the different impedance of the detector probes in the whole X band, was of the order of 3 percent.

Numerical calculations of the scattered electric field along the waveguide axis were performed for values of the real part of cylinder permittivity in the interval $1.90 \leq \varepsilon_R \leq 2.10$, and for values of the imaginary part $10^{-5} \leq \varepsilon_I \leq 10^{-1}$. The post diameters were 6.00 and 22.86 mm; frequencies in the X band and standard waveguide WR 90 (RG 52/U) were used.

The best match between the computed and measured values was reached for $\varepsilon = 2.06 - i10^{-5}$, as shown in the diagrams of Figs. 3 and 4. The values refer to the total electric field amplitude, that is, the sum of the incident and scattered field vectors.

The deviation between computed and measured values was kept within 10 percent. The comparison was made by

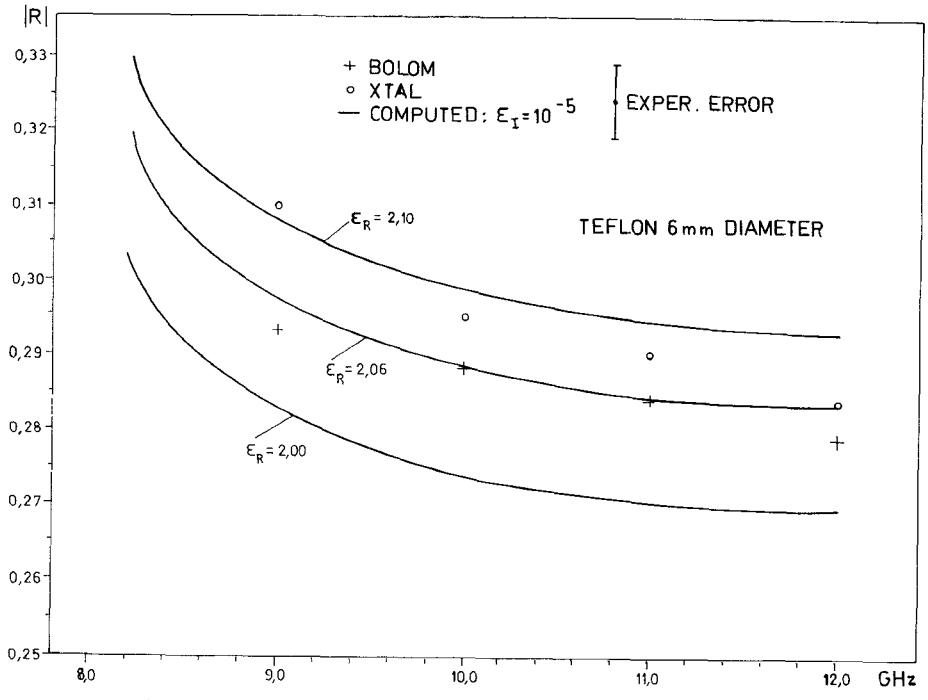

Fig. 5. Reflection coefficient amplitude versus frequency. Teflon cylinder (6-mm diameter).

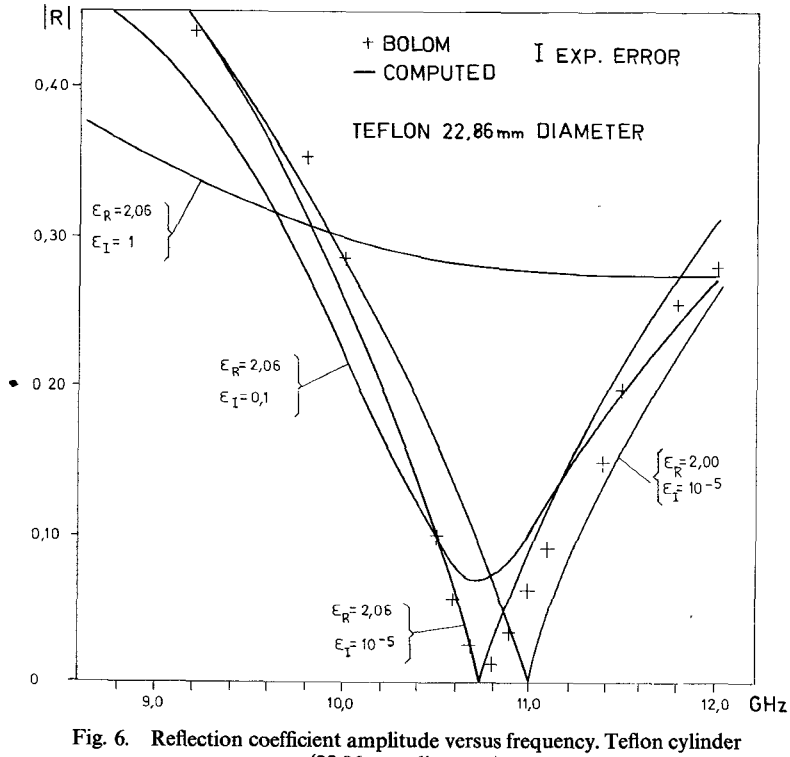

Fig. 6. Reflection coefficient amplitude versus frequency. Teflon cylinder (22.86-mm diameter).

taking into account the standing wave ratio and the first minimum position, when $2.00 \leq \varepsilon_R \leq 2.06$ and $10^{-5} \leq \varepsilon_I \leq 10^{-2}$.

In Figs. 5 and 6 the amplitudes of the reflection coefficient versus frequency are illustrated in the cases considered. For the 22.86-mm post, a resonance was detected on the frequency of 10.76 ± 0.02 GHz as a minimum of the reflection coefficient amplitude (Fig. 6). This frequency corresponds exactly to the computed value for $\varepsilon_R = 2.06$. The amplitude measured at resonance was practically zero. This behavior is in agreement with computation results when ε_I is negligible. The resonance situation allows us to

TABLE I

A) Teflon cylinder diameter 6 mm .
Frequency 10 GHz:
$\varepsilon = 2.06 - i\,10^{-5}$

$B_1 = -0{,}0864310 - i0{,}2656900$, Mod $B_1 = 0{,}279400$.
$B_2 = -0{,}0249330 + i0{,}0005103$, Mod $B_2 = 0{,}024939$.
$B_3 = (0{,}050164 + i0{,}154210)10^{-3}$ Mod $B_3 = 0{,}162170.10^{-3}$.
$B_4 = (-0{,}230520 + i0{,}004802)10^{-5}$, Mod $B_4 = 0{,}230570.10^{-5}$.
$B_5 = (0{,}062447 + i0{,}191960)10^{-7}$, Mod $B_5 = 0{,}201870.10^{-7}$.
$B_6 = (0{,}651740 - i0{,}013477)10^{-10}$, Mod $B_6 = 0{,}65188.10^{-10}$.

Test for unitary condition of the scattering matrix:

Mod $R = 0{,}28947$, Mod $T = 0{,}95690$, $(\text{Mod } R)^2 + (\text{Mod } T)^2 = 0{,}999449$.

B) Teflon cylinder diameter 22.86 mm.
Frequency 8.2 GHz,
$\varepsilon = 2.06 - i10^{-5}$

$B_1 = 0{,}334760 - i0{,}312990$, Mod $B_1 = 0{,}458292$.
$B_2 = -0{,}156300 + i0{,}937690$, Mod $B_2 = 0{,}950630$.
$B_3 = 0{,}0785330 + i0{,}073429$, Mod $B_3 = 0{,}107510$.
$B_4 = -0{,}0018428 + i0{,}011056$, Mod $B_4 = 0{,}011209$.
$B_5 = 0{,}0016098 + i0{,}0015052$, Mod $B_5 = 0{,}22038$.
$B_6 = (0{,}020352 - i0{,}122080)10^{-3}$, Mod $B_6 = 0{,}123770.10^{-3}$
$B_7 = (-0{,}18492 - i0{,}172910)10^{-5}$, Mod $B_7 = 0{,}25317.10^{-5}$
$B_8 = (-0{,}03330 + i0{,}199760)10^{-6}$, Mod $B_8 = 0{,}202510.10^{-6}$

Test for unitary condition of the scattering matrix:

Mod $R = 0{,}553567$, Mod $T = 0{,}83277$, $(\text{Mod } R)^2 + (\text{Mod } T)^2 = 0{,}999941$.

estimate the best computed measured fitting with greater accuracy. In fact, the value ε_R essentially determines the frequency of resonance, while an increase in ε_I produces an enlargement of the resonance curve and an increase in the amplitude at the resonance frequency. The sensitivity of the measurement may be computed from the shift of the resonance frequency due to the variation of ε_R by the coefficient $\delta f_0 / \delta \varepsilon_R$ which, in our case, has value of -4 GHz. A variation in ε_R from 2.06 to 2.00 shifts the resonance frequency from 10.76 to 11.00 GHz.

In Table I, the computed values of the complex amplitudes B_n for the cases illustrated in Figs. 3 and 4 are set out together with the data relevant to the test of the unitary condition for the scattering matrix. This table shows the fast convergence of the computations of the scattering field in the cases considered.

IV. Conclusion

In this paper, the solutions of the vector wave equation in cylindrical coordinates have been applied to numerical calculations of the scattered electric field in waveguide, only when the polarization of the incident wave is parallel to the cylinder axis. These solutions have been verified by comparing the measurement results obtained in experimental tests in simple cases, where homogeneous Teflon cylinders were used, with the results obtained in the calculation of the scattering coefficients carried out for a reliable value of the Teflon permittivity. The comparison shows that the formulation adopted may be considered as a suitable and powerful tool for calculations concerning plasma diagnostics [5], as well for the study of the propagation of EM fields in optic fibers where inhomogeneous dielectrics are involved.

Acknowledgment

The authors warmly thank A. P. Benedetti and P. Poli of Centro di Calcolo, C.N.E.N. in Bologna, who performed the computational programs [14].

References

[1] A. W. Adey, "Diffraction of microwaves by long metal cylinders," *Can. J. Phys.*, vol. 33, pp. 407–419, 1955.
——, "Scattering of electromagnetic waves by coaxial cylinders," *Can. J. Phys.*, vol. 34, pp. 510–520, 1956.
S. T. Wills and A. B. McLay, "Diffraction of 3,2 cm electromagnetic waves by cylindrical objects," *Can. J. Phys.*, vol. 32, pp. 372–380, 1954.
C. Froese and J. R. Wait, "Calculated diffraction patterns of dielectric rods at centimetric wavelengths," *Can. J. Phys.*, vol. 32, pp. 775–781, 1954.
M. K. Subbarao and A. B. McLay, "Diffraction of 3,2 cm electromagnetic waves by dielectric rods," *Can. J. Phys.*, vol. 34, pp. 546–554, 1956.
J. R. Wait, "The long wavelength limit in scattering from a dielectric cylinder at oblique incidence," *Can. J. Phys.*, vol. 43, pp. 2212–2215, 1965.

[2] K. J. Parbhaker and B. C. Gregory, "Plane wave interaction with an inhomogeneous warm plasma column," *Can. J. Phys.*, vol. 49, pp. 2578–2588, 1971.
[3] H. Ikegami, "Scattering of electromagnetic waves from a plasma column in a rectangular waveguide," *Jap. J. Applied Physics*, vol. 7, pp. 634–645, June 1968.
[4] N. Okamoto, I. Nishioka, and Y. Nakanishi, "Scattering by a ferrimagnetic circular cylinder in a rectangular waveguide," *IEEE Trans. Microwave Theory Tech.*, vol. MTT-19, pp. 521–527, June 1971.
[5] G. Cicconi, V. Molinari, and C. Rosatelli, "Microwave reflection from a plasma column in a rectangular waveguide," *Jap. J. Applied Physics*, vol. 12, pp. 721–734, June 1973.
[6] R. F. Harrington, *Time Harmonic Electromagnetic Fields*. New York: McGraw-Hill, 1961.
[7] R. L. Bruce, F. W. Crawford, and R. S. Harp, "A reflection technique for plasma-density measurement," *J. Applied Phys.*, vol. 39, pp. 3349–3354, June 1968.
[8] G. M. Murphy, *Ordinary Differential Equations and their Solutions*. New York: Van Nostrand, 1960.
[9] G. N. Watson, *Theory of Bessel Functions*, 2nd ed. New York: Cambridge Univ. Press, 1944.
[10] P. M. Morse and H. Feshbach, *Methods of Theoretical Physics*, Part I. New York: McGraw-Hill, 1953.
[11] E. Cupini, V. Molinari, and P. Poli, "Reflection coefficient of an electromagnetic wave by a plasma column of variable electron density in a waveguide," *Alta Frequenza*, vol. XLII, pp. 62–68, Feb. 1973.
[12] R. F. Harrington, *Field Computation by Moment Methods*. New York: Macmillan, 1968.
[13] G. Cicconi and C. Rosatelli, "Alcuni Metodi di Calcolo Numerico in Problemi di Diffusione di Microonde da Ostacoli Cilindrici," *Alta Frequenza*, vol. XLII, pp. 41–51, Jan. 1973.
[14] A. P. Benedetti and P. Poli, "REFLEX: A programme to calculate the scattering by a plasma column in a rectangular waveguide," Comitato Naz. Energia Nucleare. RT/FIMA (75)3, 1975.

Some Effects of Field Perturbation upon Cavity-Resonance and Dispersion Measurements on MIC Dielectrics

P. H. LADBROOKE

Abstract—**An analysis is presented of field perturbations in MIC resonators in order to examine the errors which occur in permittivity measurements made by cavity-resonance methods: Q factor, coupling effects, fringing fields, crystal misalignment (for anisotropic materials), and changes in ambient temperature are all considered. Analysis of a cavity with mixed boundary conditions shows that the resonant-mode frequencies depend to the first order on that part of Q_0 associated with imperfect electric (metal) walls, but to the second order on that part associated with imperfect magnetic (open-circuit) walls. A new expression is given for the Q of an open-ended microstrip resonator when surface waves are excited in the dielectric, and it is shown that the unloaded Q (Q_0) can be dominated by this phenomenon. It is further shown that these Q-related effects, together with reactive perturbations arising from fringing and coupling structures, are the principal source of error in measurements for ε or ε_{eff}. Such reactive effects may be treated semiquantitatively by applying Slater's perturbation theorem to the affected region. These procedures lead to the following revised values for the crystal permittivity of sapphire (monocrystalline Al_2O_3) in the microwave region: $\varepsilon_{\|}$ (parallel to the c axis) = 11.6; $\varepsilon_{\perp}$ (base-plane) = 9.4.**

I. Introduction

ALTHOUGH alumina (ceramic Al_2O_3) finds more widespread application in hybrid microwave integrated circuits than does sapphire (monocrystalline Al_2O_3), sapphire offers the following advantages (against which one must offset its higher cost): i) its electrical properties are exactly repeatable from sample to sample; ii) it can be polished optically flat, which means that lower loss circuits of greater precision can be constructed by thin-film techniques; iii) it is transparent, so it is possible to align optically a "flipped" device chip for bonding directly into a microstrip circuit without the parasitic inductance of bond wires; iv) it is compatible with silicon epitaxial technology (SOS). Given these kinds of application, the need to measure the dielectric properties of either substrate material at microwave frequencies is clear.

A number of papers have been published dealing with test structures which can be made by thin-film metallizing the substrate itself, leading either to the permittivity ε directly [1]–[4], to an effective permittivity ε_{eff} in the case of microstrips [5], or to some secondary variation such as the temperature coefficient $(1/\varepsilon)(\partial\varepsilon/\partial T)$ [6]. All of these test circuits were, and still are, in the nature of cavity resonators with one dimension thin ($\ll\lambda$), often with mixed boundary conditions (i.e., some electric walls, some magnetic walls). The object was in every case to retrieve the permittivity from cavity-resonance measurements made upon the structure, using the relationship [7]

$$\varepsilon = \frac{c^2}{f_{n,m}^2}\left\{\left(\frac{n}{2y_1}\right)^2 + \left(\frac{m}{2z_1}\right)^2\right\} \tag{1}$$

Manuscript received February 17, 1976; revised December 3, 1976.
The author is with the Department of Solid State Electronics, University of New South Wales, Kensington, Australia 2033.